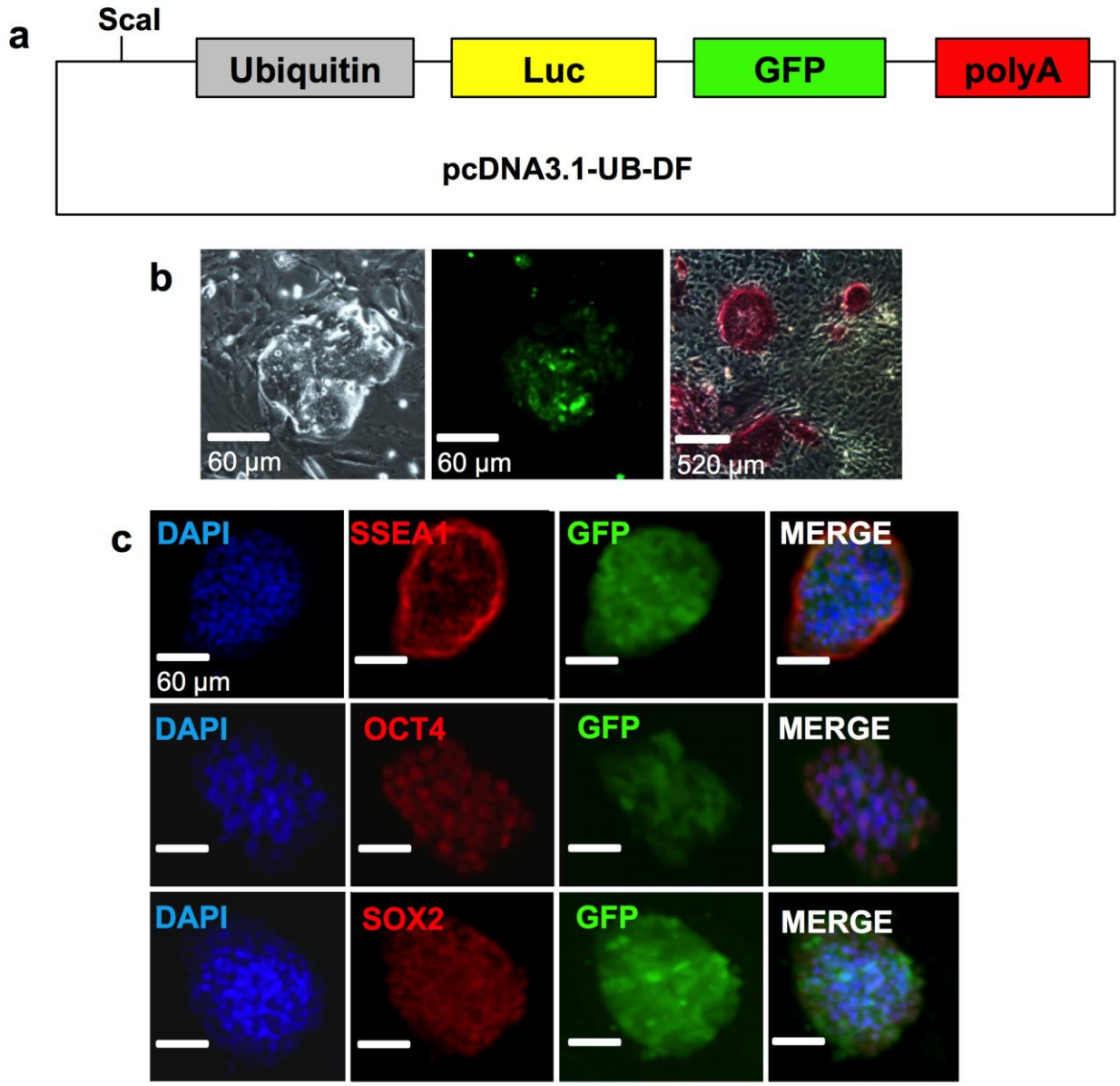

Supplementary Fig. 1. Characterization of lentiviral-reprogrammed iPSC line derived from a GFP-Luciferase transgenic FVB mouse fibroblast. **(a)** Map of the plasmid carrying GFP and luciferase (Luc) genes under control of the ubiquitin promoter. **(b)** Undifferentiated iPSCs had typical ESC-like colony morphology (left), expressed GFP (mid), and alkaline phosphatase (AP). **(c)** iPSCs stably expressed the embryonic markers such as SSEA1, Oct4, and Sox2.

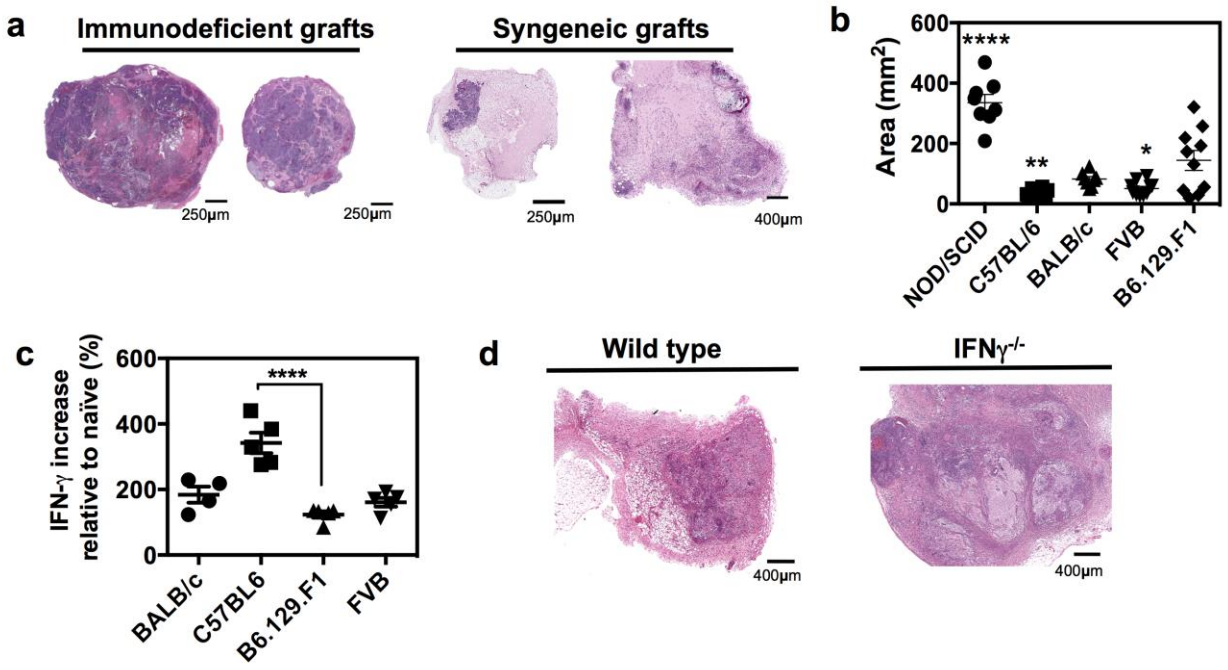

Supplementary Fig. 2. Immunological rejection of lentiviral-derived syngeneic iPSCs is not due to reporter transgene expression. (a) Two representative histopathological sections (H&E) of B6.129.F1 iPSC (free of GFP and luciferase expression) grafts per group explanted from immunodeficient (left; 1x magnification) and syngeneic mice (right; 5x magnification). Data are representative of at least 9 animals and 3 independent experiments. (b) iPSC graft areas measured 30 days post-intramuscular injection of iPSCs in immunodeficient (NOD/SCID), allogeneic (BALB/C, C57BL6, FVB), and syngeneic (B6.129.F1) mice. Data are representative of mean ± s.e.m. of at least 8 animals per group from 2 independent experiments. (c) IFN-γ ELISPOT demonstrating the percent production of IFN-γ by syngeneic (B6.129.F1) and allogeneic primed splenocytes (from BALB/c, C57BL/6, and FVB) relative to the respective naïve splenocytes in response to iPSCs (B6.129.F1). Data are representative of mean ± s.e.m. of 5 mice per group. (d) Histopathological views of iPSC grafts harvested 30 days after implantation in syngeneic C57BL/6 wild-type or C57BL/6 IFN-$\gamma^{-/-}$ mice. Significance of differences between series of results was assessed using ANOVA with Tukey for multiple comparisons. *$p<0.05$, **$p<0.01$, ***$p<0.001$, ****$p<0.0001$.

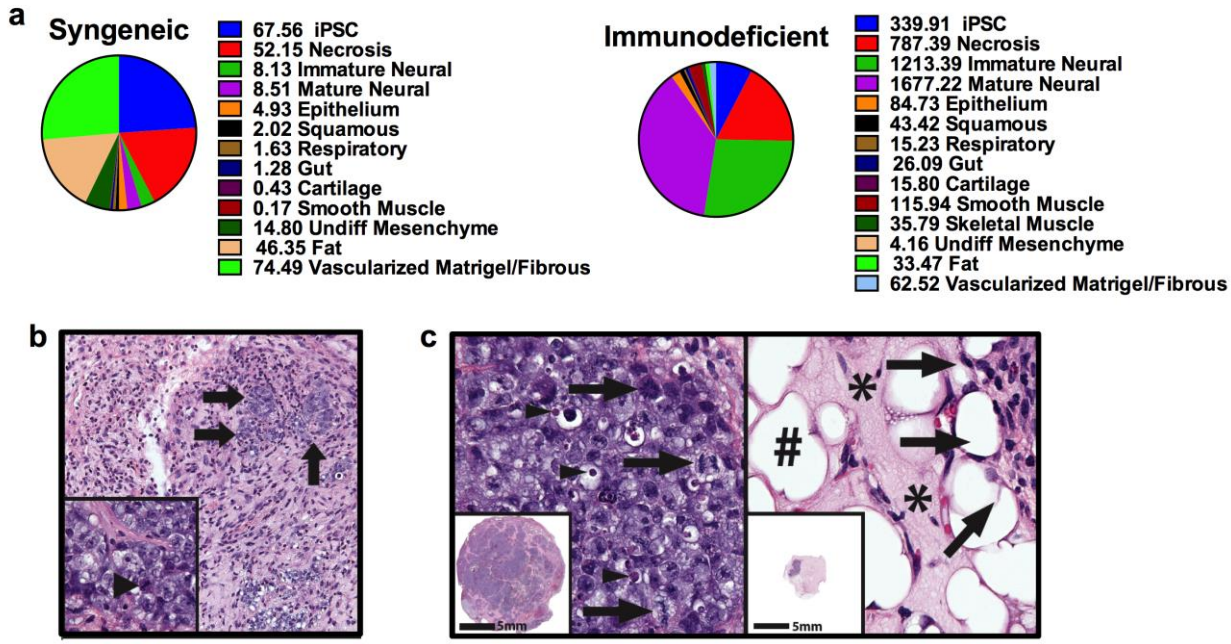

Supplementary Fig. 3. Undifferentiated iPSCs were still present in the grafts at the time of immunological analysis. **(a)** Pie charts demonstrating the dimensions of the areas (mm^2) in which the listed cell types occupied grafts extracted from syngeneic (n=10) and immunodeficient (n=6) mice 14 days post-implantation. **(b)** A syngeneic iPSC graft extracted from mouse at 14 days post-implantation demonstrate the presence of undifferentiated cells (arrows). iPSCs were identifiable based on high nuclear-to-cytoplasmic ratios, frequent mitotic features (arrow head, inset), and the absence of any morphologic evidence of differentiation. **(c)** iPSCs injected into immunodeficient mice formed large subcutaneous tumors that persist for at least 30 days post-implantation (left panel, inset). These cells were identifiable based on high nuclear-to-cytoplasmic ratios, frequent mitotic features (arrows) and apoptotic bodies (arrowheads), and the absence of any morphologic evidence of differentiation. In contrast, iPSCs injected into syngeneic wild-type mice were mostly eliminated, resulting in much smaller tumors (right panel, inset) comprising predominantly of pauricellular Matrigel (right panel, *) and adipocytes (#) with lymphohistiocytic infiltrate (demarcated by arrows).

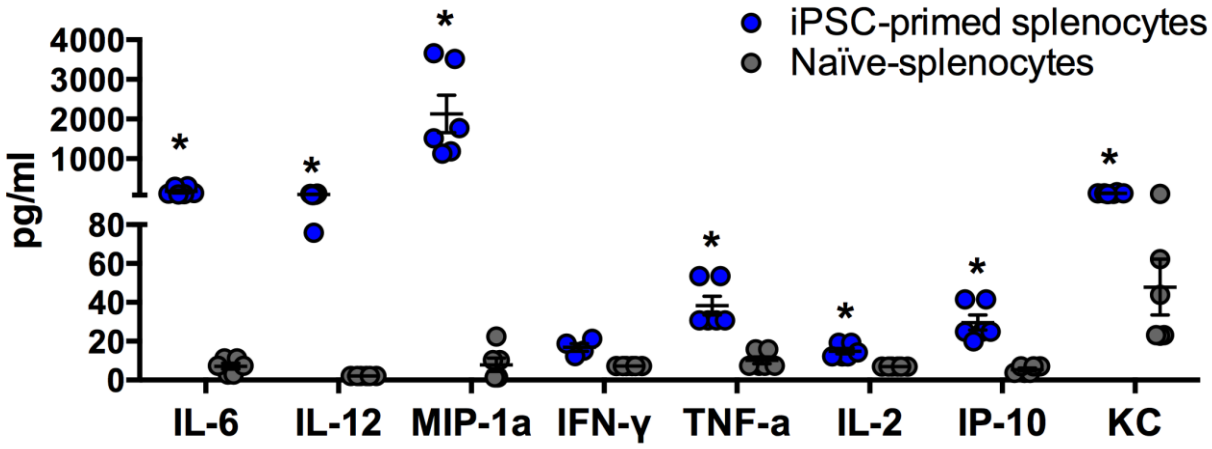

Supplementary Fig. 4. Syngeneic iPSCs elicit a pro-inflammatory immune response when co-cultured with syngeneic iPSC-primed splenocytes *in vitro*. Splenocytes ($2x10^5$) isolated from mice (n=6) primed with syngeneic iPSCs (10^5) or splenocytes from naïve mice (n=6) were co-cultured with syngeneic iPSCs for 76 hr *in vitro*. Various pro-inflammatory cytokines were measured in the culture supernatant by Luminex. Data are representative of mean ± s.e.m. of 6 mice per group. Significance of differences between series of results was assessed using two-tailed unpaired Student *t*-test. * $p<0.05$.

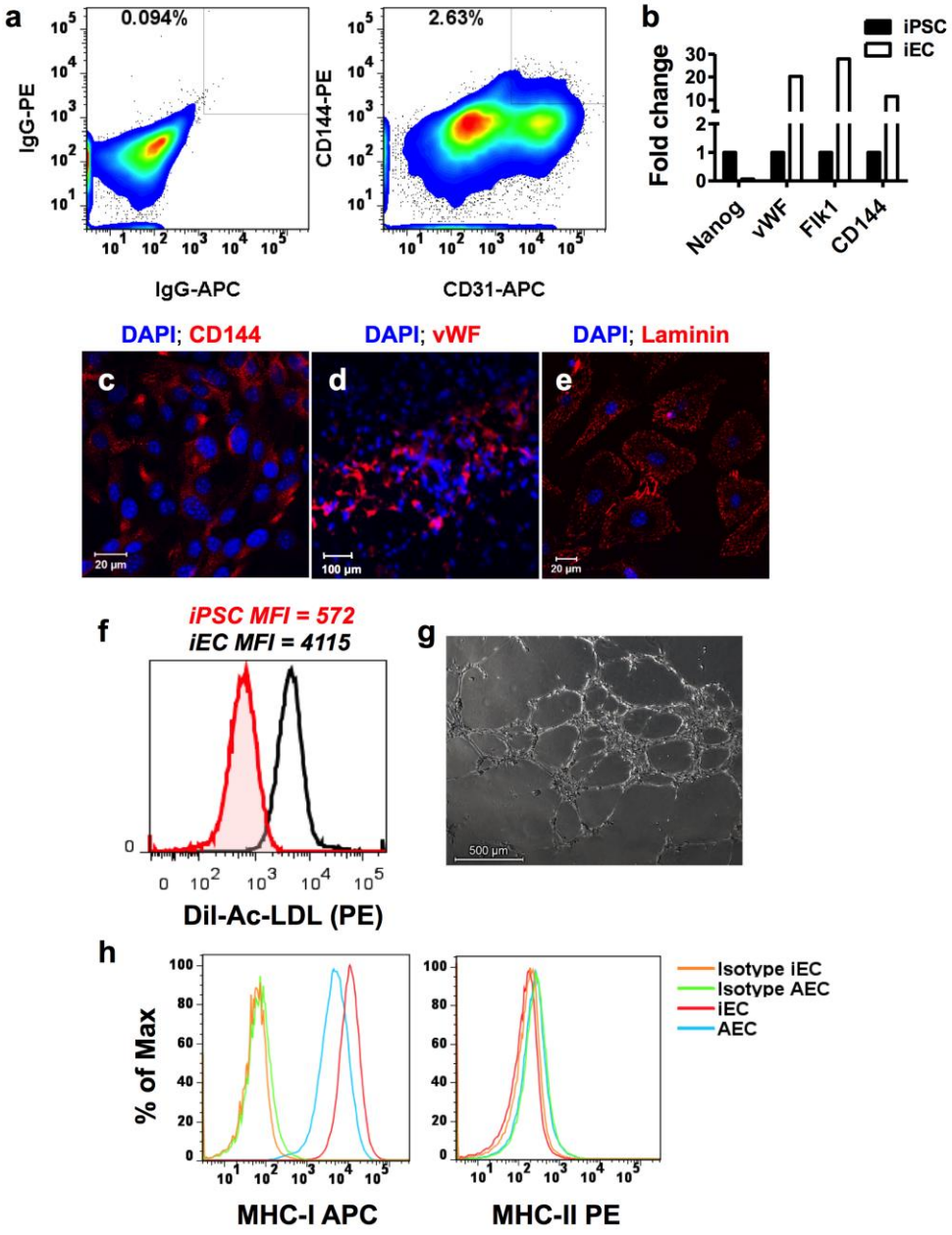

Supplementary Fig. 5. Purification and characterization of iECs. **(a)** Gating strategy for purification of differentiated iECs ($CD144^{+}/CD31^{+}$) by FACS. **(b)** Fold-change in transcript expression relative to undifferentiated iPSCs. Purified iECs showed up-regulation of endothelial transcripts (vWF, Flk1, CD144) as well as down-regulation of the pluripotency marker Nanog, consistent with terminal differentiation to endothelial lineage. Endothelial phenotype was characterized by immunofluorescence staining of endothelial-specific markers such as **(c)** CD144 and **(d)** von Willebrand factor. Functional phenotype of iECs was characterized by the production of **(e)** extracellular matrix laminin, **(f)** uptake of low-density protein, and **(g)** angiogenesis by means of tube-formation assay. **(h)** Expression of MHC-I and MHC-II in iECs and AECs by FACS.

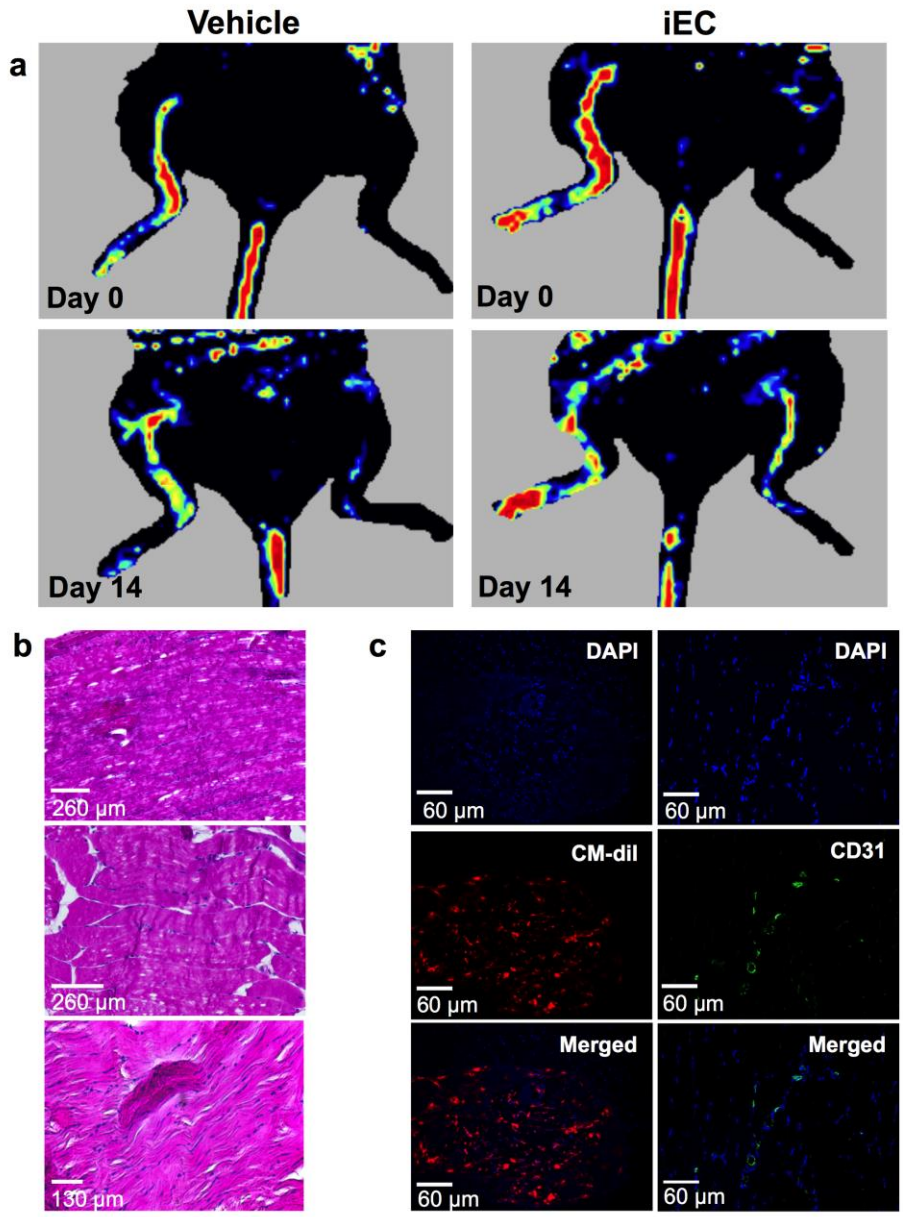

Supplementary Fig. 6. In a model of ischemia injury, iECs engrafted and promoted re-vascularization of the hindlimb of immunodeficient mice without any evidence of tumor formation. **(a)** Laser Doppler imaging of blood perfusion 1 hr after left hindlimb ischemia demonstrate a severe reduction of blood flow in mice treated with vehicle or iECs injection (top panels). Hindlimbs of mice at 14 days post-ischemia (bottom panels) demonstrate iEC injection promoted re-vascularization compared to control vehicle injection. **(b)** Histological evaluation of ischemic hindlimb at 14 days after iEC injection. No evidence of tumor formation was found in iEC grafts. **(c)** Immunofluorescence staining of hindlimbs at 14 days after iEC injection. CM-DiI labeled (red; left panel) iECs show localization and survival of iECs in the ischemic hindlimbs. Cell surface staining for CD31 (green) demonstrate structural organization of iECs in vascular-like structures.

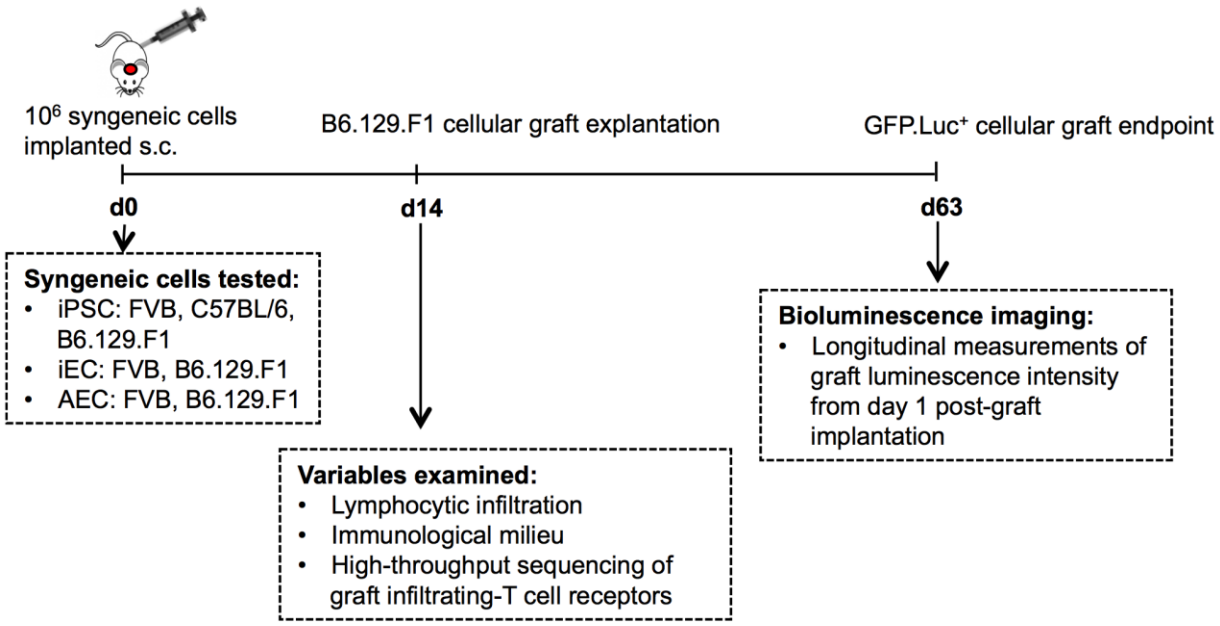

Supplementary Fig. 7. Schema of experimental design used to assess the immunogenicity of iPSC, iECs, and AECs.

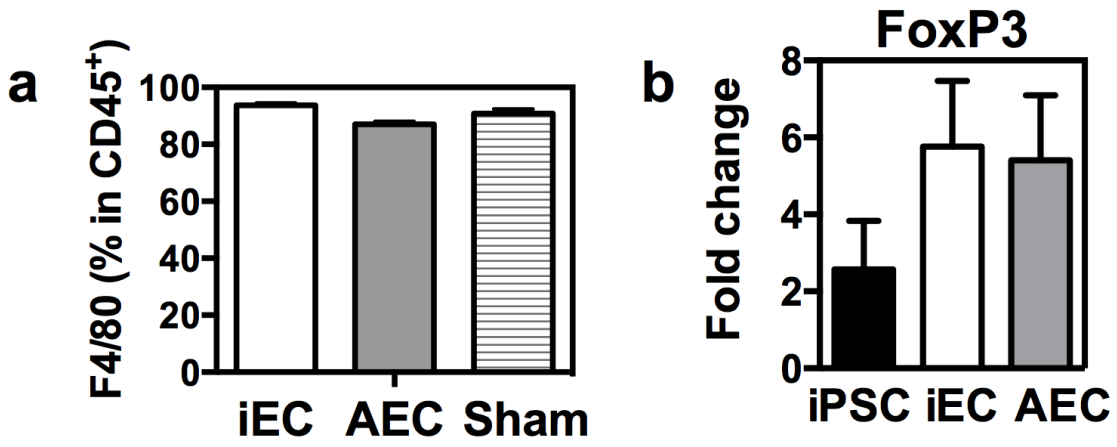

Supplementary Fig. 8. Assessment of macrophage infiltration and FoxP3 mRNA expression in different grafts. **(a)** Macrophages represented the predominant immune cell population infiltrating iEC, AEC, and sham grafts. Macrophage ($F4/80^+$) infiltration was quantified by FACS. Data are representative of mean ± s.e.m. of 5 animals per group. **(b)** Fold-change in FoxP3 expression relative to sham grafts demonstrating no differences between iPSC, iEC, and AEC grafts. Data are representative of mean ± s.e.m. of eight animals per group.

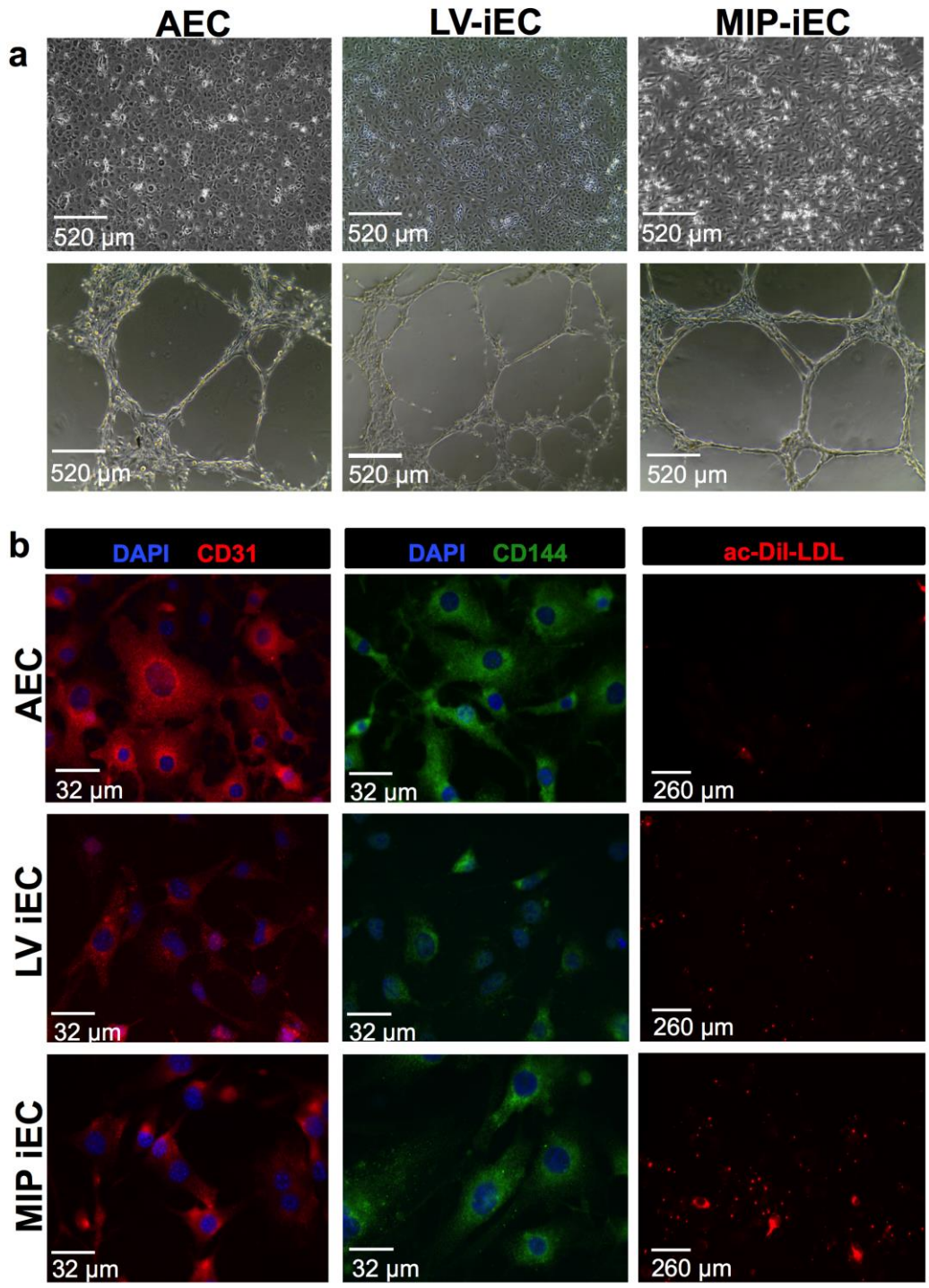

Supplementary Fig. 9. Characterization of murine induced pluripotent stem cell-derived endothelial cells (iECs). **(a)** Brightfield overview of aortic endothelial cells (AEC), lentiviral-derived endothelial cells (LV-iEC), and mini-intronic plasmid-derived endothelial cells (MIP-iECs) (top panel). Formation of tube-like structures on Matrigel characteristic of endothelial cells (bottom panel). **(b)** Nuclear staining with DAPI (blue) and cell surface staining for CD31 (red) and CD144. Uptake of ac-Dil-LDL (red) by endothelial cells.

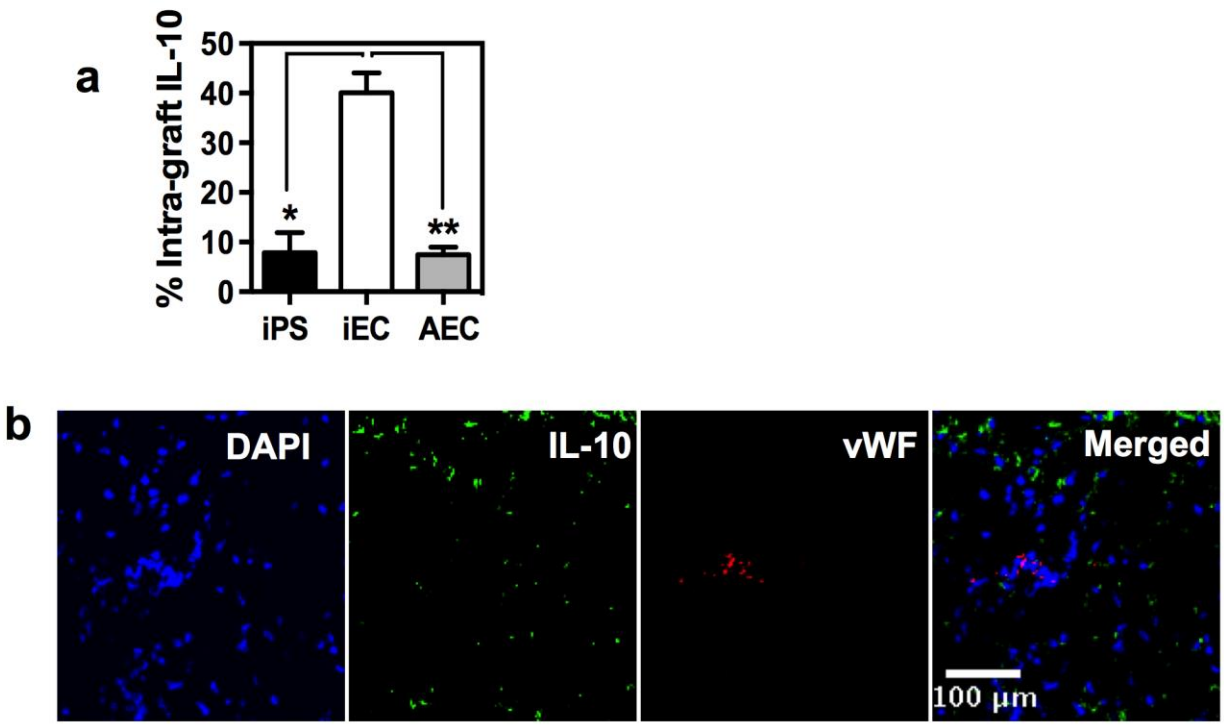

Supplementary Fig. 10. IL-10 in iEC grafts originated from cellular infiltrates. **(a)** Quantification of IL-10 expression was performed in 5 random fields from each graft type (40x magnitude). **(b)** IL-10 expression was not associated with endothelial cells. Von Willebrand factor (vWF) was used to label endothelial cells and to determine association with IL-10. Data are representative of mean ± s.e.m. of a minimum of 1,000 cells from 5 randomly selected fields. Significance of differences between series of results was assessed using ANOVA with Tukey for multiple comparisons. *p<0.05, **p<0.01, ***p<0.001, ****p<0.0001.

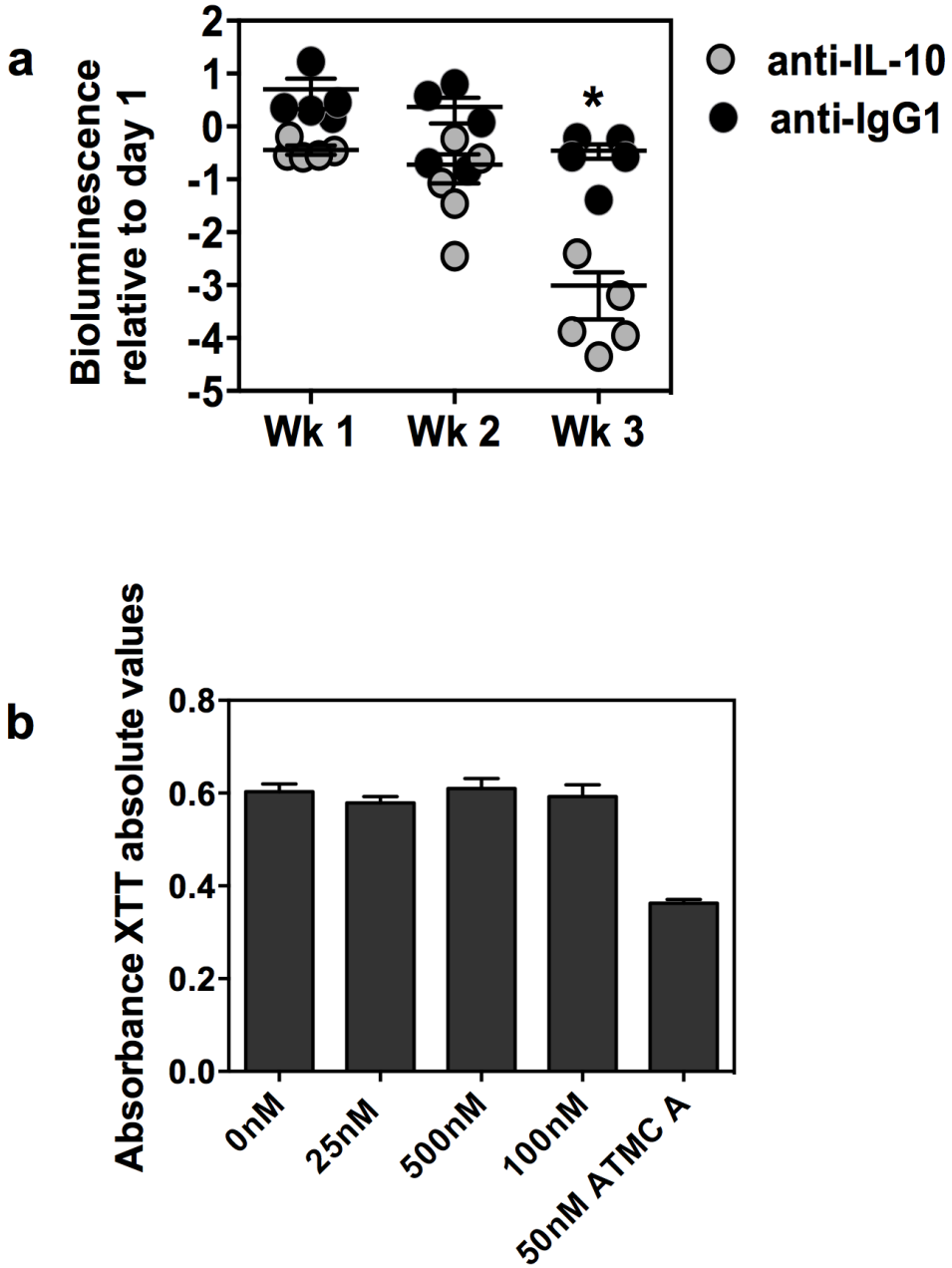

Supplementary Fig. 11. Neutralization of IL-10 promoted rejection of iECs in syngeneic recipients. **(a)** Longitudinal survival of iECs was monitored in syngeneic mice by means of bioluminescence imaging. Data are representative of mean ± s.e.m maximum bioluminescence radiance relative to day 0 (n=5). Significance of differences between series of results was assessed using two-tailed unpaired Student *t*-test. Antibody-based neutralization of IL-10 promoted loss of iEC's bioluminescence signal within 3 weeks of cell implantation, consistent with cell death due to immune rejection. **(b)** Anti-IL-10-mediated cytotoxicity was examined in iECs *in vitro*. Data are representative of mean ± s.e.m of 3 technical replicates.

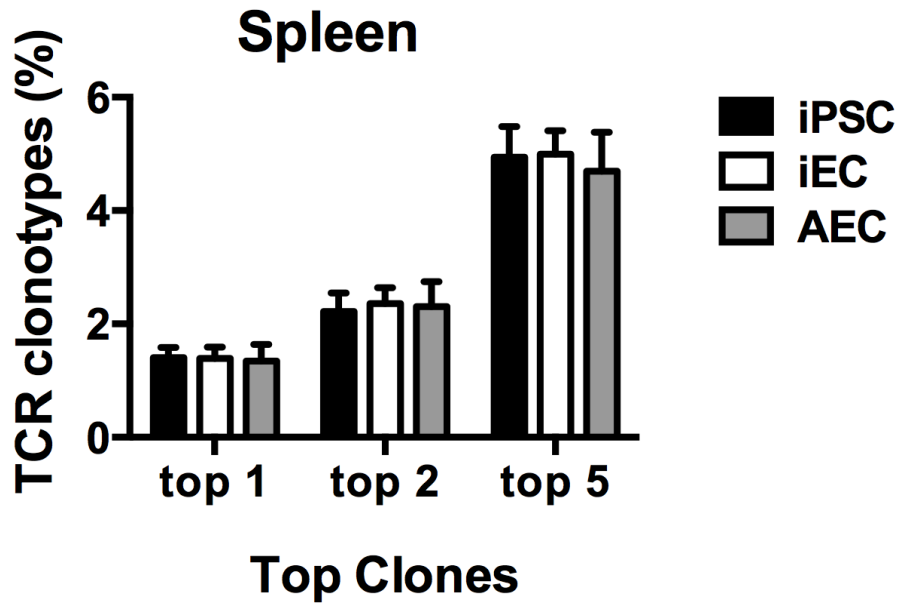

Supplementary Fig. 12. T cell repertoire of spleens from mice with iPSC, iEC, and AEC grafts. Contrary to T cells infiltrating iPSC grafts, splenic T cells of mice with iPSC grafts showed no repertoire skewing. Data are representative of mean ± s.e.m of 3 mice per group and two independent experiments.

Supplementary Table 1. Genes found to be significantly up-regulated in iEC compared to iPSC grafts.

Symbol	Unigene	Refseq	Description
Ccl3	Mm.1282	NM_011337	Chemokine (C-C motif) ligand 3
Cdk2	Mm.111326	NM_016756	Cyclin-dependent kinase 2
Csf1	Mm.795	NM_007778	Colony stimulating factor 1 (macrophage)
Fas	Mm.1626	NM_007987	Fas (TNF receptor superfamily member 6)
Fos	Mm.246513	NM_010234	FBJ osteosarcoma oncogene
Foxp1	Mm.234965	NM_053202	Forkhead box P1
Icam1	Mm.435508	NM_010493	Intercellular adhesion molecule 1
Il10	Mm.874	NM_010548	Interleukin 10
Il7r	Mm.389	NM_008372	Interleukin 7 receptor
Ing4	Mm.262547	NM_133345	Inhibitor of growth family, member 4
Jak1	Mm.289657	NM_146145	Janus kinase 1
Mef2a	Mm.132788	NM_001033713	Myocyte enhancer factor 2A
Nfatc3	Mm.383185	NM_010901	Nuclear factor of activated T-cells, cytoplasmic, calcineurin-dependent 3
Nfkb1	Mm.256765	NM_008689	Nuclear factor of kappa light polypeptide gene enhancer in B-cells 1, p105
Notch1	Mm.290610	NM_008714	Notch gene homolog 1 (Drosophila)
Stat3	Mm.249934	NM_011486	Signal transducer and activator of transcription 3
Stat6	Mm.121721	NM_009284	Signal transducer and activator of transcription 6
Tgfb1	Mm.248380	NM_011577	Transforming growth factor, beta 1
Tnfrsf10b	Mm.193430	NM_020275	Tumor necrosis factor receptor superfamily, member 10b

Supplementary Table 2. Number of TCR clones (among the top 50 most prevalent clones) shared between different graft types. Data is representative of two independent experiments (Exp 1 and Exp 2).

	Shared TCR clones													
Comparison	**Exp1**	**Exp1**	**Exp1**	**Exp1**	**Exp2**	**Exp2**	**Exp2**	**Exp2**	**Exp2**	**Exp2**	**Exp2**	**Exp2**	**Exp2**	**Mean ± s.e.m**
iPSC to iPSC	3				5	3								3.7 ± 0.4
iPSC to iEC	0	1	3	4	4	7	0	4	10	0	2	1	5	3.1 ± 0.3
iPSC to AEC	7	5	0	4	0	0	6	4	2	6	5	0	0	3.0 ± 0.3
iEC to iEC	12				6	8								8.7 ±1.0
iEC to AEC	11	8	8	16	12	8	15	15	6	19	10	5	11	11.1 ± 0.5
AEC to AEC	15				8	14								12.3 ± 1.3